Large round cell granulomas induced by murine sarcoma virus (Moloney) in mouse brains

Kenji Jinno[*]

[*]Okayama University,

Large round cell granulomas induced by murine sarcoma virus (Moloney) in mouse brains[*]

Kenji Jinno

Abstract

The effect of murine sarcoma virus of Moloney strain on central nervous system was examined morphologically in Swiss mice of different age. A single intracranial inoculation of cell-free virus solution resulted in the induction of characteristic intracerebral granulomas in 82.8% of the newborn to 5 day-old group, in 71.4% of the 6 to 10 day-old group, and in 68.0% of the 11 to 20 day-old group. The mean latency periods to tumor recognition were 16.5, 21.1, and 33.5 days, respectively. The granuloma consisted of inflammatory cell infilrations, reactive gliosis, and richly developed blood vessels. The lesions consistently contained numerous characteristic large round cells. In cases of long-survival, the findings included reparative changes, such as extensive gliosis, withdrawal of inflammation, and a decrease in the numbers of large round cells and blood vessels. These lesions were tentatively designated as "large round cell granuloma." The early foci of the granoloma were composed of proliferating glial cells and large round cells at the subependymal regions. Electron microscopically these large round cells had abundant intracytoplasmic fibrils quite similar to gliofibrils. Numerous C-type virus particles were present in the intercellular nad perivascular spaces, and occasionally budded from cell membranes of the large round cells and vascular endothelia. The large round cells were considered to be reactive astrocytes activated by biral infection. It was conclided that MSV-M was not a sarcomogenic but a granulomogenic virus in mice. Control animals showed no pathological changes.

LARGE ROUND CELL GRANULOMAS INDUCED BY MURINE SARCOMA VIRUS (MOLONEY) IN MOUSE BRAINS

Kenji JINNO

*Department of Pathology, Okayama University Medical School,
Okayama, Japan (Director : Prof. K. Ogawa)*

Received for publication, March 18, 1975

Abstract : The effect of murine sarcoma virus of Moloney strain on central nervous system was examined morphologically in Swiss mice of different age. A single intracranial inoculation of cell-free virus solution resulted in the induction of characteristic intracerebral granulomas in 82.8% of the newborn to 5 day-old group, in 71.4% of the 6 to 10 day-old group, and in 68.0% of the 11 to 20 day-old group. The mean latency periods to tumor recognition were 16.5, 21.1, and 33.5 days, respectively. The granuloma consisted of inflammatory cell infiltrations, reactive gliosis, and richly developed blood vessels. The lesions consistently contained numerous characteristic large round cells. In cases of long-survival, the findings included reparative changes, such as extensive gliosis, withdrawal of inflammation, and a decrease in the numbers of large round cells and blood vessels. These lesions were tentatively designated as "large round cell granuloma." The early foci of the granuloma were composed of proliferating glial cells and large round cells at the subependymal regions. Electron microscopically these large round cells had abundant intracytoplasmic fibrils quite similar to gliofibrils. Numerous C-type virus particles were present in the intercellular and perivascular spaces, and occasionally budded from cell membranes of the large round cells and vascular endothelia. The large round cells were considered to be reactive astrocytes activated by viral infection. It was concluded that MSV-M was not a sarcomogenic but a granulomogenic virus in mice. Control animals showed no pathological changes.

In 1966, murine sarcoma virus of Moloney strain (MSV-M) was isolated from leukemic mice previously inoculated with the Moloney leukemic agent (1). Hartley and Rowe (2) demonstrated that the cell-free extracts of tumors induced by MSV-M produced altered cell foci in tissue cultures of mouse embryo fibroblasts. The oncogenicity of the virus and the morphology of the virus-induced tumor in mesenchymal tissues have been extensively investigated in mice (3-12), rats (13-16), and hamsters (14, 17). In the central nervous system, hemangioendothelioma, meningioma, and gliomas were induced in rats by intracranial injection of MSV-M (18-26). In mice, this injection resulted in capillary hemangioma and glioma (20). However, in the

291

292   K. Jinno

mice study (20), the virus-induced intracerebral lesions were not morpholo-
gically investigated in fine detail. In the present study, the author examines
(a) the histogenesis of intracerebral lesions in mice by light and electron
microscopy and (b) the histological differences of the intracerebral lesions
following virus inoculation at different age periods.

MATERIALS AND METHODS

Virus preparations. Tumor tissues produced by vertically transmitted MSV-
M in the soft parts of mice were obtained by courtesy of Dr. N. Ida of
Toyokogyo Hospital, Hiroshima. The tumor tissues were minced with a scis-
sor, suspended in physiologic saline, and filtered using a two-layered gauze.
About 2 weeks after intramuscular inoculation of the tumor cell suspension to
newborn Swiss mice, the transplanted tumors were excised and pooled at
$-70°C$. A 25% W/V suspension of the pooled tumor tissues was allowed to
digest in 0.2 M phosphate-buffered saline (PBS) containing 1 mg of hyaluro-
nidase per 100 ml for 1 hr at room temperature; freeze-thawed repeatedly; and
homogenized in a teflon-headed type of homogenizer. The homogenate was
clarified twice by low-speed centrifugation ($2300 \times g$, 20 min) and then centri-
fuged at $10,000 \times g$ for 30 min at $-4°C$. Supernatants were pipetted off, anti-
biotics (streptomycin $100 \mu g/ml$, penicillin 500 units/ml) added, and the solution
was stored at $-70°C$ until use as the inoculum (MSV-2). These procedures
were essentially a modification of the Moloney procedure for purification of
the virus (27).

Normal muscular tissues from adult mice of the same strain were excised
and treated by the same methods as those for the tumor tissues. These materials
were used as the inoculums for the control group.

Virus titration. The virus fluid was diluted with PBS in tenfold series.
Newborn Swiss mice were inoculated intramuscularly with each virus dilution
and observed until death. The 50% lethal dose per 0.02 ml (LD50/0.02 ml) was
calculated by the Reed-Muench's method (28). Virus stocks had titer of $10^{0.7}$LD
50/0.02 ml.

Animals. One hundred and forty-seven male and female mice of the Swiss
strain were used. They were obtained from the inbred colony of Okayama
University Medical School. All the animals were fed a balanced diet of MF
pellets (Oriental Yeast Industrial Company, Tokyo) and kept in metal con-
tainers with wire mesh covers. Water was freely available from suckling
bottles.

Groups and Treatments. The animals were divided into 4 experimental and
1 control group.

Group I: Thirty-four mice within 5 days after birth were inoculated intra-
cranially in the center of the right cerebral hemisphere using a tuberculin
syringe. The dose administered was 0.02 ml of the virus fluid. The inoculation
procedures were the same in all other groups.

Group II: Thirty-nine mice from 6 to 10 days of age were inoculated with
0.02 ml of the virus fluid.

Group III: Fifty-five mice from 11 to 20 days of age were inoculated with 0.03 ml of the virus fluid.

Group IV: Adult mice were given 0.05 ml of the virus fluid.

Control group: Seven newborn mice were inoculated with 0.02 ml of the extract from normal muscular tissues.

For examining the early stages of virus-induced lesions, a total of 24 mice from Groups I, II, and III were successively killed at 3 to 7 day intervals for about 4 weeks after virus inoculation.

Moribund or ill mice with various symptoms were killed by perfusing the central nervous system with 10% neutral buffered formalin solution using a wing-webbed needle to the left ventricle of the heart, or by removing the calvarias under ether anesthesia.

The brain and other organs were examined macroscopically and fixed in 10% buffered formalin solution for light microscopy. Four brain slices were prepared by sagittal sections through one median and 2 paramedian lines. They were embedded in paraffin.

Light microscopy. Hematoxylin-eosin stainings were performed on all the specimens. In addition, the Matsumoto silver impregnation method for reticulum fiber, Bodian method for nerve fiber, Mallory's Azan, phosphotungstic acid hematoxylin (PTAH), Klüver-Barrera, Giemsa, Berlin blue, and Holzer's glial fiber stainings were selectively used.

Electron microscopy. To 6 day-old mice, 0.02 ml of the virus fluid was inoculated intracranially. The animals were sacrificed when symptoms appeared. They were anesthesized by ether inhalation and the calvarias were removed as soon as possible. The brains were cut in coronal sections and small, diced pieces of the lesion were prepared and fixed with cold buffered 3% glutaraldehyde solution (pH 7.2) for 1.5 hr. Post-fixation with 2.5% buffered osmium tetraoxide was performed for 1 hr. After rinsing with Millonig's buffer, the specimens were dehydrated in graded concentrations of ethanol and embedded in Epoxy resin. Ultrathin sections of the representative areas were cut with a Porter-Blum MT-2 ultramicrotome with glass knives. These sections placed on copper grids were double stained with uranyl acetate and lead citrate and examined with a Hitachi HS-8 electron microscope at an accelerating voltage of 50 kv.

RESULTS

1. *Symptoms, incidences, latency periods, and distributions of the virus-induced lesions*

A total of 116 mice survived after virus inoculation for more than 10 days. In Group I, 24 of 29 mice (82.8%) developed granulomas with characteristic large round cells. The mean latency period for granuloma recognition was 16.5 days (Table 1). Almost all mice in Groups I and II became moribund or died by 20 days after virus inoculation. In Group II, the incidence of granulomas was 20 of 28 (71.4%) and the average letency period was 21.1

Table 1. Incidence of intracerebral large round cell granulomas in
mice inoculated with MSV-M

| Experimental groups	Inoculation day after birth	Inoculum (ml)	Mean latency period (day)	Total no. of mice	Incidence of intracerebral granuloma (%)
Group I	1 to 5	MSV-2 0.02	16.5	29 M 13 F 16	24 (82.8) M 11 (84.6) F 13 (81.2)
Group II	6 to 10	MSV-2 0.02	21.1	28 M 17 F 11	20 (71.4) M 12 (70.6) F 8 (72.7)
Group III	11 to 20	MSV-2 0.03	33.5	47 M 26 F 21	32 (68.0) M 17 (65.4) F 15 (71.4)
Group IV*	adult	MSV-2 0.05	211 to 322**	12 M 8 F 4	0
Control group	newborn	control fluid*** 0.02	20 to 167**	7 M 4 F 3	0

M, male; F, female.
* One case of lymphosarcoma was found.
** Observation period without neurological symptoms.
*** Extract from normal muscular tissues.

days. In Group III, the incidence was 32 of 47 mice (68.0%) and the latency period was 33.5 days. The lesions in Group III were small and restricted to the subependymal zones except in a few cases.

Almost all granulomas were multicentric in origin and distributed at the subependymal regions, predominantly along the walls of the olfactory and
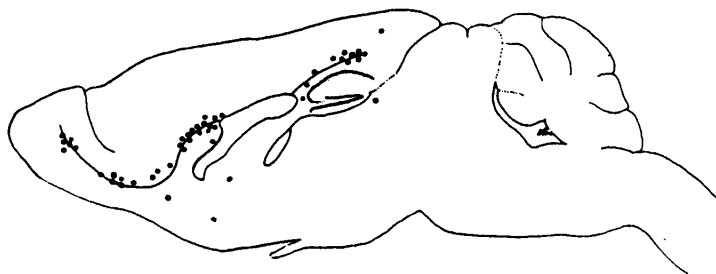
Text-Fig. 1. Schematic representation of predilection sites in mice for the development of MSV-M-induced intracerebral granuloma. The chart shows the localization of 47 early foci of granulomas found in the paramedian sagittal planes of the cerebrum in 31 mice of Groups I and II. These early foci often showed multicentric localizations.

lateral ventricles, or at the tapetums which were in contact with the hippo-campus. Some lesions were found randomly in the cortex (Text-Fig. 1).

Seventy-six mice which developed granuloma in the brain showed re-tarded development, loss of body weight, ruffled hair, cranial enlargement, and languid activity. Observed neurological symptoms included paralysis of hind- or forelegs, ataxia, rotatory movement, hyperexcitability, and lethargy (Fig. 1). The latency period between virus inoculation and the appearance of symptoms ranged from 8 to 32 days (average, 15.2 days) in Group I. This mean value coincided closely with the time of granuloma recognition. This relationship was also present in Groups II and III. How-ever, very few neurological symptoms were observed in Group III animals.

2. *Macroscopical findings of the brain*

Subcortical petechial bleeding sometimes associated with intraventri-cular hemorrhage was the most common finding in animals inoculated by MSV-M (Fig. 2). Swellings of the cerebral hemispheres, yellowish necrotic areas, hydrocephalus, and cerebral defects were also seen at various frequen-cies (Fig. 3). On cut-surfaces, brownish or greyish areas were found with hemorrhages in the deeper part of the cerebrum (Fig. 4), corresponding to the microscopical lesions. These findings were most prominent in Group I.

3. *Histological findings of the cerebral lesions*

In Group I, the virus-induced lesions were highly cellular, well demar-cated from adjacent neural tissues, and occasionally hemorrhagic (Fig. 5). The lesions had a tendency to extend along the ventricle (Fig. 6).

The four essential histological components of lesions (Figs. 7, 8) common to Groups I, II and III were:

A. Numerous characteristic large round cells
B. Prominent vascular proliferation
C. Inflammatory cell infiltration, predominantly polymorphonuclear neutrophils and monocytes
D. Reactive gliosis

Initially, a number of characteristic large round cells appeared through-out the lesion (Figs. 9, 10, 11). The abundant cytoplasms of these large round cells were moderately eosinophilic and of homogeneous character, sometimes having small vacuoles. The relatively clear nucleus was also large, with prominent amphophilic nucleolus and some of the nuclei were located in the center of the cytoplasm. Very often, the nucleus was slightly pycnotic and was found at an eccentric position in the cytoplasm; at these times the cytoplasm appeared more eosinophilic. There were some degenerating large round cells that showed weakly stained vacuolated cytoplasm and a more

pycnotic nucleus. Such large round cells were sparse and separately scattered in many instances. A few smaller cells were also present. No definite glial fibers were stained with PTAH staining or the Holzer method. With the Bodian method no argyrophilic fibers were noted in the large round cells. The cytoplasms were stained light-purple with the Klüver-Barrera method and no Nissl bodies were noted. PAS-positive substance was not present in the cytoplasm. The Matsumoto method did not show reticulum fibers around individual large round cells (Figs. 12, 13). Mitotic figures were extremely rare. In neural tissues adjacent to the lesions, the large round cells were scattered sparsely. They usually had one nucleus and sometimes two nuclei. However, the multinucleated giant cells were not seen. Several large round cells engulfed cell debris and neutrophils.

The number of large round cells decreased with time after the peak of granuloma development, i. e., at about 17 to 20 days after virus inoculation in Groups I and II.

Secondly, tortuous vascularity was conspicuous; collapsed or dilated blood vessels of various sizes were proliferated in many portions of the lesion. The vessels were lined by a layer of swollen and spindle-shaped endothelial cells often with fibrin thrombi. Small hemorrhagic foci, fibrin deposition, and aggregations of neutrophils were seen around the small vessels. Sections stained with Mallory's Azan and the Matsumoto method revealed collagen and reticulum fibers around perivascular connective tissues with extensions into the lesions. Sometimes, reticulum networks deriving from these connective tissues were extensive.

The number of the blood vessels decreased with time as the large round cells decreased, and the endothelia became flattened.

Thirdly, there was a severe, diffuse or focal cellular exudate consisting of numerous polymorphonuclear neutrophils, monocytes, and a few round cells (Fig. 14). Hemosiderin stained blue by Berlin blue stainings was frequently phagocytosed by monocytes in the hemorrhagic areas. Occasionally these cells had foamy cytoplasms.

Fourthly, proliferations were found of polygonal or fusiform astrocytes having fine cytoplasmic processes and an oval nucleus with fine chromatin structure (Figs. 15, 16, 17). In these areas, abundant neuroglial fibers were demonstrated with the Holzer method and PTAH staining (Fig. 18). Arrangements of astrocytes were anisomorphic in many areas, isomorphic at some areas, and often surrounded the large round cells and blood vessels.

In Groups I and II, these glial proliferations were intensive and extensive with time after the peak of inflammation at about 17 to 20 days after inoculation. They were, therefore, most prominent in the long-survival cases. In

Group III, glial proliferations were present without an elapse of severe inflammatory changes. In the adult group and the control group such lesions were not found in the brain.

The neighboring parenchymal tissues of the brains were severely edematous and the degenerated nerve cells were sparsely separated. The ependymal layers were involved in the granulomatous lesions at times, and the ependymal cells were reactively proliferated.

Besides the intracerebral lesions, a tumorous kind of lesion of the meninges was observed composed of compactly proliferated fibroblasts in 12 mice (Fig. 19).

4. *Sequential observations on morphogenesis of the intracerebral lesions*

During the first several days after virus inoculation, slight inflammatory tissue damage was found transiently from the injection needle. In Groups I and II, the earliest lesion that could be detected showed a proliferation of astrocytes and a few spongioblasts with several large round cells (Figs. 20, 21). These changes appeared at the subependymal zones of the olfactory and lateral ventricles of both cerebral hemispheres. The average latency period for these changes was 12.0 days in Group I (early stage). Thereafter, inflammatory cells, mainly polymorphonuclear neutrophils, began to infiltrate in the form of perivascular cuffings at the same sites (Figs. 22, 23). Simultaneously, the proliferation of capillaries occurred and progressed with the appearance of numerous large round cells and with extensive migrations of polymorphonuclear neutrophils and monocytes. In Group I, these events were completed by an average latency period of 16.9 days and often resulted in a lethal outcome (florid stage).

In one mouse in Group I at postinoculation day (PID) 22, the fascicular arrangement of large or small spindle cells was seen in close contact with the ependymal layer, but these cells did not show any relationship to the wall of the blood vessels.

In two Group I mice at PID 28 and 32, that survived the florid stage, reactive gliosis occurred extensively accompanied by the withdrawal of inflammation, and a decreased number of large round cells and blood vessels was observed (Figs. 15, 16, 17). The endothelia of the blood vessels became flattened (reparative stage). These findings were also present in Group II.

In Group II, the latency periods for the early and florid stages were PID 15.6 and 18.6, respectively. In 12 mice of Group II, the florid stage was apparent. However, in Group III, this stage was not seen; periventricular glioses were extended gradually with a few large round cells and slight inflammatory cell infiltration. In 7 mice, the reparative stage was found on the mean PID 39.6. In other mice in Group III, the lesions of the early

298   K. JINNO

stages did not advance remaining at the subependymal layers.

5. Electron microscopic findings of the intracerebral lesions

   Varieties of cellular compositions were found electron microscopically that confirmed the light microscopy. The large round cells were irregularly round or oval-shaped (Fig. 24). Frequently, the nucleus was eccentrically located in the cytoplasm with a conspicuous, dense nucleolus. The nuclear envelope was prominently invaginated on one side where the Golgi apparatus were located. The cytoplasm was large but well preserved. A characteristic cytoplasmic feature was the presence of abundant fine fibrils about 70–90 Å in width, quite similar to glial fibrils (Fig. 25). Randomly oriented and intermingled fibrils filled the cytoplasm almost completely. However, in the periphery of the cytoplasm, the fibrils were straight for some distance and frequently showed parallel arrangement. The slightly dilated rough-surfaced endoplasmic reticulum was relatively developed in the periphery and a low electron-dense content was present in the cisternae. A number of Golgi apparatus, numerous free ribosomes, ribosomal rosettes, and a few lysosomes were also observed. Several mitochondria were seen in the peripheral cytoplasm (Fig. 26). No parallel rough-surfaced endoplasmic reticulum (Nissl granule) and microtubules were present in the cytoplasm. There were no collagen fibers in the intercellular spaces of the large round cells.

   Electron microscopic examinations of the lesions easily revealed a large number of extracellular virus particles measuring about 120–130 nm (Fig. 27). The extracellular virus particles seen most frequently were characterized by an electron-dense nucleoid with a diameter of about 70–80 nm surrounded by a double membrane. Some of virus particles were composed of distinct shells with electron-lucent nucleoid and were observed in the promixity of the cell membrane. Budding of the virus particles from the cell membrane of the large round cells was occasionally observed (Fig. 28). These virus particles were morphologically identical to C-type RNA virus particles. They were distributed around the large round cells, in the degenerated amorphous areas with the cell debris, and between the cell membrane of the vascular endothelium and basal lamina (Figs. 29, 30). A few virus particles and budding viruses were also seen in the lumen of the blood vessels (Fig. 31). Occasionally virus particles were seen within vacuoles of the large round cells and endothelia. These virus particles might be pinocytosed by the cells (Fig. 32).

   There was infiltration of numerous monocytes, occasionally with phagocytosed erythrocytes (Figs. 33, 34). The polymorphonuclear leukocytes were also seen in the degenerated or hemorrhagic areas. The endothelia of capillaries had an irregularly infolded large nucleus with dense chromatin on the inner nuclear membrane. Their cytoplasms were relatively swollen with

numerous ribosomes and the cytoplasms were extended with many thin processes in the lumen, so that the vascular lumens was narrow.

DISCUSSION

Ribacchi and Girald (18, 19) intracerebrally injected newborn rats with murine sarcoma virus, Moloney's strain. These animals after 18 to 27 days developed leptomeningeal hemangioendothelioma, meningioma, and glioblastoma. Of 46 brains examined in these studies, multifocal hemangioendotheliomas were found associated with one meningioma and with 15 glioblastomas. Glioblastoma arose mostly from the periventricular subependymal tissues and were composed of large cells. Ida *et al.* (29, 30) recovered the virus after serial transplantation of sarcoma that developed in newborn mice exposed to intrauterine infection with MSV-M. According to their reports, tumors developed in new-born rats and mice intracranially inoculated with the virus. The mean latency period of tumor appearance for rats was 26 days (20-22) and for mice, 18 days (20). Most of these tumors showed either capillary hemangiomas or gliomas, and several tumors appeared to be gemistocytic astrocytomas.

In the present study of mice intracerebral lesions, the author noticed the coexistence in the same lesion of numerous characteristic large round cells with blood vessels and the infiltration of various inflammatory cells. Furthermore, reparative change with gliosis was observed, indicating the granulomatous character of the lesions.

It was difficult to determine the exact cell origin of the large round cells in this study, but they seemed to be of glial cell origin : these cells appeared at the subependymal regions quite far from the brain surface at the early stages ; the intercellular reticulum fibers derived from individual large round cells were absent ; and electron microscopy showed the presence of abundant fine fibrils in the cytoplasm. These fibrils seemed to be identical with glial fibrils demonstrated in other virus-induced gliomas (31-34). It seemed unlikely that the large round cells were derived from perivascular cells. In the parenchyma of the mouse brain, few adventitial cells were found around blood vessels, except at the larger vessels in the neighborhood of the pia mater ; these adventitial cells could not be transformed into the large round cells of the present study, which appeared at the deeper part of the brain. Kitamura *et al.* (35), using autoradiographic electron microscopy, suggested that the so-called pericytes which were reported to migrate and to transform into macrophages were migrating leucocytes under extravasation. Since " proper pericytes " do not migrate, the large round cells often appearing at distant sites from the blood vessels were not considered as originating from pericytes. Furthermore,

300   K. Jɪɴɴᴏ

the ultrastructure of the large round cells differed from migrating monocytes in that the large round cells had few lysosomes and abundant fibrillar structures.

It seemed likely that subependymal glial cells had the ability to develop to large round cells, since at the early stages these cells were consistently present with the proliferating glial cells at the subependymal regions without any particular correlation with the blood vessels. The importance of subependymal cells for the development of some experimental brain tumors has often been pointed out (31, 36, 37, 38, 39, 40). It is also of interest that human subependymal giant cell astrocytomas, often seen in tuberous sclerosis, appear at the paraventricular zone (41). These reported findings along with the results of this study suggest that specific glial cells at subependymal zones may be sensitive to various stimuli, such as virus, or that virus particles have a tendency to gather at the periventricular zones from the route of the interstitial humoral fluids of the brain. The features of the large round cells were analogous to those of the large ballooned cells in human subependymal giant cell astrocytomas.

The large round cells in this study were extremely similar to those observed in Rous sarcoma virus (RSV)-induced mammalian brain tumors (31, 40, 42) and MSV-M-induced rat brain tumors (18, 20-22, 26). In the RSV-induced brain tumor, the light and electron microscopic findings of " huge round cell " in " huge round-celled tumor " reported by Kumanishi *et al.* (31) were very similar morphologically to the large round cells of this study, in findings such as the presence of large cytoplasm, abundant fine fibrillar structures, and other organelles. These investigators have also suggested the glial cell origin of the " huge round cell " based upon morphological and isozymal studies. In MSV-M-induced rat brain tumor, Ida *et al.* (26) established a continuous tissue culture line that originated from rat brain tumor and examined the electron microscopic features of cultured cells. In their study, the cultured cells possessed few gliofibrils and some features were similar to oligodendrocytes. However, occasional cultured cells had abundant gliofibrils. Most, if not all, of the large round cells in this study also had abundant fine fibrils. These experimental results and the morphological similarities of the large round cells to large cells in other RNA virus-induced intracerebral lesions would also suggest that the large round cells might be of glial, especially astrocytic origin. However, further examination will be necessary to determine the exact cell origin of the large round cells of this study.

In mice at least, the proliferation of the large round cells was self-limiting. The cells did not show neoplastic proliferations, and they decreased in number in the long-survival cases. Degenerating cells were also ob-

served.   These findings suggested that the large round cells were non-neoplastic.   They might disappear in mice before a neoplastic change could be induced.

In 1964, Harvey (43) described a murine sarcoma virus (MSV-H) that was isolated during routine passage of Moloney's leukemic virus, using plasma collected from leukemic rats.   Although it is generally assumed that the Harvey (MSV-H) and Moloney (MSV-M) strains are similar, morphological differences were studied between mesenchymal tumors induced by these two viruses (10, 11).   It was reported by Duffy (44) that the injection of MSV-H directly into the brain of newborn mice resulted in the development of highly vascular sarcomas, in which the endothelia were at times arranged in multiple laminae and were often seen extending into the surrounding masses of tumor cells.   In the present study, vascular proliferation was prominently seen in places, but it was a granulomatous self-limiting process. There was no evidence of sarcomatous change of the endothelia.

The lesions induced in the soft parts of mice by MSV-M have been reported as different morphological entities by different investigators, i. e., rhabdomyosarcoma (3-5), undifferentiated sarcoma (6), mesenchymal sarcoma (12), and atypical granuloma (8, 9).   Ferer et al. (7), Berman et al. (10), and Siegler (12) noticed the inflammatory reaction characteristically associated with these sarcomas.   The inflammatory changes in these reports were considered to be a reaction to the growth of the sarcoma.   However, Stanton et al. (9) classified most mesenchymal tumors induced in mice by MSV-M as " atypical granuloma " rather than neoplasia.   Simons and McCuly (11) have described the lesions as a benign, reparative inflammation.   These latter concepts are supported by the result in this study of intracerebral lesions.   The meningeal lesions in this study were identical morphologically with mesenchymal tumors induced by MSV-M.

C-type virus particles were often present around the large round cells. Budding viruses from the plasma membrane, viropexis, and intracytoplasmic virus particles were also observed in these cells.   These findings would suggest that the large round cells had a close relationship to C-type virus.   The glial cells might be transformed into large round cells by virus invasion and acquire a virus-producing activity.   The virus particles might be MSV-M or endogeneous latent virus naturally present in mice activated by MSV-M.   The former would be more plausible, because the cell-free extract of the MSV-M induced tumor tissues could almost always reproduce the same tumors.

In the present study, viremia was electron microscopically evident from the virus particles present in the vascular lumen of the intracerebral granuloma.   These particles might be pinocytosed by the basal plasma membranes

302   K. JINNO

and discharged out into the lumen of the blood vessels across capillary walls along with the humoral fluid. Budding viruses were also demonstrated from the luminal surfaces of the endothelia.

It is conceivable that the mouse brain tissues were activated, degenerated, and destroyed concurrently by MSV-M, and following reparative changes, a peculiar histological picture of intracerebral granuloma resulted. It must be concluded that MSV-M in mice was not sarcomogenic but a granuloma-producing virus.

REFERENCES

1. Moloney, J. B.: The application of studies in murine leukemia to the problems of human neoplasia. In *Some Recent Developments in Comparative Medicine*, ed. R. Fiennes, pp. 251-258, Academic Press Inc., London, 1965.
2. Hartley, J. W. and Rowe, W. P. : Production of altered cell foci in tissue culture by defective Moloney sarcoma virus particles. *Proc. Natl. Acad. Sci.* 55, 780-786, 1966.
3. Perk, K. and Moloney, J. B.: Pathogenesis of a virus induced rhabdomyosarcoma in mice. *J. Natl. Cancer Inst.* 37, 581-599, 1966.
4. Dalton, A. J.: An electron microscopic study of a virus-induced murine sarcoma (Moloney). *Nat. Cancer Inst. Monograph* 22, 143-168, 1966.
5. Perk. K., Moloney, J. B. and Jenkins, E. G.: Further studies on the relationship of a rhabdomyosarcoma virus to muscle tissue. *Int. J. Cancer* 2, 43-52, 1967.
6. Chirigos, M. A., Scott, D., Turner, W. and Perk, K.: Biological, pathological and physical characterization of a possible variant of a murine sarcoma virus (Moloney). *Int. J. Cancer* 3, 223-237, 1968.
7. Ferer, A., McCoy, J. L., Perk, K. and Glynn, J. P.: Immunologic, virologic and pathologic studies of regression of autochthonus Moloney sarcoma virus-induced tumors in mice. *Cancer Res.* 28, 1577-1585, 1968.
8. Law, L. W., Ting, R. G. and Stanton, M. F.: Some biologic, immunogenic and morphologic effects in mice after infection with a murine sarcoma virus. I. Biologic and immunogenic studies. *J. Natl. Cancer Inst.* 40, 1101-1112, 1968.
9. Stanton, M. F., Law, L. W. and Ting, R. C.: Some biologic, immunogenic, and morphologic effects in mice after infection with a murine sarcoma virus. II. Morphologic studies. *J. Natl. Cancer Inst.* 40, 1113-1129, 1968.
10. Berman, L. D. and Allison, A. J.: Studies on murine sarcoma virus ; a morphological comparison of tumorigenesis by the Harvey and Moloney strains in mice, and the establishment of tumor cell lines. *Int. J. Cancer* 4, 820-836, 1969.
11. Simons, P. J. and McCuly, D. J.: Pathologic and virologic studies of tumors induced in mice by two strains of murine sarcoma virus. *J. Natl. Caucer Inst.* 44, 1289-1303, 1970.
12. Siegler, R.: Pathogenesis of virus-induced murine sarcoma. I. Light microscopy. *J. Natl. Cancer Inst.* 45, 135-147, 1970.
13. Perk, K., Shachat. D. A. and Moloney, J. B.: Pathogenesis of a rhabdomyosarcoma

(undifferentiated type) in rats induced by a murine sarcoma virus (Moloney). *Cancer Res.* **28**, 1197-1206, 1968.

14. Soehner, R.L. and Domochowski, L.: Induction of bone tumors in rats and hamsters with murine sarcoma virus and their cell-free transmission. *Nature* **224**, 191-192, 1969.

15. Ikemoto, K. and Fukushima, A.: Comparison of MSV-M-induced osteogenic sarcoma. *Proc. Jap. Cancer Assoc.*, 33rd Annu. Meet., p. 130, 1974.

16. Tanaka, K., Yoshida, T. and Tanaka, T.: Establishment of a virus-persistent cell line and deviation of malignant cell clones from osteosarcoma induced by a murine sarcoma virus (Moloney). *Gann* **63**, 459-469, 1972.

17. Huebner, R.J., Hartley, J.W., Rowe, W.P., Lane, W.T. and Capps W.I.: Rescue of the defective genome of Moloney sarcoma virus from a non-infectious hamster tumor and the production of pseudotype sarcoma viruses with various leukemia viruses. *Proc. Natl. Acad. Sci.* **56**, 1164-1169, 1966.

18. Ribacchi, R. and Giraldo, G.: Intracranial tumors in rats injected intracerebrally with murine sarcoma virus (MSV-M), Moloney's strain. Preliminary report. *Lab. Anat. Pat. Perugia.* **26**, 141-148, 1966.

19. Ribacchi, R. and Giraldo, G.: Plasmacytomas occurring in the bones of rats injected intracerebrally with murine sarcoma virus (MSV), Moloney's strain. Preliminary report. *Lab. Anat. Pat, Perugia.* **26**, 149-156, 1966.

20. Ida, N., Ikawa, Y., Ogawa, K., Takada, M. and Yokoki, E.: Intracranial tumors in rats and mice produced by MSV-CS-Moloney substrain. *Proc. Jap. Cancer Assoc.*, 29th Annu. Meet., p. 97, 1970.

21. Ida, N.: About the vertical transmission of leukemogenic viruses—Sarcomogenic viruses and virus-induced brain tumors. *Nihon Rinsho* **29**, 1468-1484, 1971 (in Japanese).

22. Ida, N., Ikawa, Y., Sugano, H. and Ogawa, k.: Pathological and biological findings of MSV-M induced rat brain tumors and their cell culture line. *Proc. Jap. Cancer Assoc.*, 30th Annu. Meet., p. 49, 1971.

23. Ida, N., Takada, M. and Ogawa, K.: Cell culture lines originated from MSV-M induced rat brain tumors and focus formation assay. *Proc. Jap. Cancer Assoc.*, 30 th Annu. Meet., 59, 1971.

24. Moriwaki, Y. and Takada, M.: Chromosome study of cultured cell line derived from MSV-Moloney induced rat brain tumors. *Proc. Jap. Cancer Assoc.*, 30th Annu. Meet., p. 59, 1971.

25. Ogawa, K.: Transplantation of cultured cell line originated from MSV-CS-Moloney induced rat brain tumor and induction of bone tumor with its cell-derived MSV. *Proc. Jap. Cancer Assoc.*, 30th Annu. Meet., p. 60, 1971.

26. Ida, N., Ikawa, Y., Ogawa, K., Takada, M. and Sugano, H.: Cell culture from a rat brain tumor induced by intracerebral inoculation with murine sarcoma virus. *J. Natl. Cancer Inst.* **53**, 431-447, 1974.

27. Moloney, J.B.: Biological studies on a lymphoid-leukemia virus extracted from sarcoma 37. I. Origin and introductory investigations. *Bibl. Haematol.* **36**, 221-233, 1969.

28. Reed, L.J. and Muench, H.: A simple method of estimating fifty percent endpoints. *Am. J. Hyg.* **27**, 493-497, 1938.

29. Ida, N., Ikawa, Y. and Ohba, Y.: Studies on hypodiploid and hyperdiploid virus-induced mouse leukemias and the vertical transmission of MSV-Moloney. *Bibl. Haematol.* **36**, 221-233, 1969.

30. Ida, N., Ikawa, Y., Ohba, Y. and Yamada, S.: Vertical transmission of MSV-Moloney in Swiss ICR mice. *Abstracts of the 10th Int. Cancer Congr.*, p. 163, 1970.

31. Kumanishi, J., Ikuta, F. and Yamamoto, T.: Brain tumors induced by Rous sarcoma virus, Schmidt-Ruppin strain. III. Morphology of brain tumors induced in adult mice.

304   K. Jinno

J. Natl. Cancer Inst. **50**, 95–109, 1973.

32. Bucciarelli, E., Rabotti, G. F. and Dalton, A. J.: Ultrastructure of gliomas induced in hamsters with Rous sarcoma virus. *J. Natl. Cancer Inst.* **38**, 865–889, 1967.

33. Vick, N. A., Bigner, D. D. and Kvedar, J. P. : The fine structure of canine gliomas and intracranial sarcomas induced by the Schmidt-Ruppin strain of the Rous sarcoma virus. *J. Neuropathol. Exp. Neurol.* **30**, 354–367, 1971.

34. Haguenan, F., Rabotti, G. F., Lyon, G. and Moraillon, A.: Gliomas induced by Rous sarcoma virus in the dog—an ultrastructual study. *J. Natl. Cancer Inst.* **46**, 539–559, 1971.

35. Kitamura, T. and Fujita, S.: Cells of reticuloendothelial system in the brain and their relationship to circulating leukocytes, microglia and pericytes. Recent Advances in RES Research. *Jap. Soc. RES.* **13**, 48–60, 1973.

36. Zimmerman, H. M.: The nature of gliomas as revealed by animal experimentations. *Am. J. Pathol.* **31**, 1–29, 1955.

37. Hopewell. J. W, and Wright, E. A.: The importance of implantation site in cerebral carcinogenesis in rats. Cancer Res. **29**, 1927–1931, 1969.

38. Bigner, D. D., Odom, G. L., Mahaley, M. S., Jr. and Day, E. D.: Brain tumors induced in dogs by the Schmidt-Ruppin strain of Rous sarcoma virus : Neuropathological and immunological observations. *J. Neuropathol. Exp. Neurol.* **28**, 648–680, 1960.

39. Ogawa, K., Hamaya, K., Fujii, Y., Matuura, K. and Endo, T.: Tumor induction by adenovirus type 12 and its target cells in the central nervous system. *Gann* **60**, 383–392, 1969.

40. Rabotti, G. F., Anderson, W. R. aud Sellers, R. L.: Oncogenic activity of Mill-Hill (Harris) strain of Rous sarcoma virus for hamsters. *Nature* **206**, 946–947, 1965.

41. Rubinstein, L. J. : *Tumors of the Central Nervous System*, pp. 40–42, A. F. I. P., Washington, D. C., 1972.

42. Rabotti, G. F. and Raine, W. A.: Brain tumors induced in hamsters inoculated intracerebrally at birth with Rous sarcoma virus. *Nature*. **204**, 898–899, 1964.

43. Harvey, J. J.: An unidentified virus which causes the rapid production of tumors in mice. *Nature* **204**, 1104, 1964.

44. Duffy, P. E.: Virus induced cerebral sarcoma. *J. Neuropathol. Exp. Neurol.* **29**, 370–391, 1970.

Legends to Figures

Fig. 1. A general view of mouse injected intracranially with MSV-M. Note cranial enlargement and paralysis of hind legs. Postinoculation day (PID) 15 from Group I.

Figs. 2-4. Gross findings of the brains.

Fig. 2. Note multiple subcortical hemorrhagic foci. PID 32 from Group II.

Fig. 3. Note prominent swelling of the right cerebral hemisphere. PID 18 from Group II.

Fig. 4. Note hemorrhagic foci on the cut-surface. PID 16 from Group I.

Fig. 5. The virus-induced intracerebral lesions (arrows) at the lateral and olfactory ventricles. PID 17 from Group I. H.E. ×12.

Fig. 6. Note the extension of the lesion (arrows) along the ventricle. PID 16 from Group I. H.E. ×12.

Figs. 7-23. Light microscopic findings of the virus induced intracranial lesions.

Fig. 7. Intracerebral granuloma. Note the complicated histological picture composed of proliferated blood vessels, large round cells, glial cells, and infiltrated inflammatory cells. PID 18 from Group II. H.E. ×100.

Fig. 8. Intracerebral granuloma. PID 16 from Group I. H.E. ×100.

Fig. 9. Intracerebral granuolma. Note the characteristic large round cells with abundant cytoplasm and large nucleus with prominent nucleolus. The nucleus is located eccentrically in the cytoplasm. PID 17 from Group I. H.E. ×400.

Fig. 10. Intracerebral granuloma. Note increase in acidophility and small vacuoles in the cytoplasm of the large round cells. PID 17 from Group I. H.E. ×200.

Fig. 11. Intracerebral granuloma. Note the scattered large round cells distant from the capillary. PID 18 from Group I. H.E. ×100.

Fig. 12. Intracerebral granuloma. Reticulum stain reveals no newly formed reticulum fibers deriving from individual large round cells. PID 17 from Group I. Matsumoto silver impregnation. ×200.

Fig. 13. Intracerebral granuloma. Note the absence of reticulum fibers between the large round cells (arrows). PID 16 from Group I. Matsumoto silver impregnation. ×400.

Fig. 14. Intracerebral granuloma. Note diffused or focal infiltration of inflammatory cells, predominantly polymorphonuclear neutrophils and monocytes. Small hemorrhagic focus (arrow) is also seen. PID 17 from Group I. H.E. ×200.

Fig. 15. Intracerebral granuloma. Note the prominent proliferation of astrocytes and a decrease in the number of large round cells. PID 29 in Group II. H.E. ×100.

Fig. 16. Intracerebral granuloma. Note the prominent proliferation of glial cells associated with the narrowing of the vascular channels and a decrease in the number of large round cells. PID 28 from Group I. H.E. ×200.

Fig. 17. Intracerebral granuloma. Glial proliferation is intensive. Note withdrawal of inflammatory cells and the flattened endothelia. PID 28 from Group I. H.E. ×400.

Fig. 18. Intracerebral granuloma. Note the intensive proliferation of glial fibers. PID 32 from Group I. Holzer. ×400.

Fig. 19. Meningeal lesion. Note the fascicular arrangement of fibroblasts. H.E. ×200.

Fig. 20. Early stage of intracerebral granuloma. Note the small band-shaped focus at the tapetum along the ventricle. The focus is composed of a few large round cells, astrocytes, and a few spongioblasts. PID 13 from Group II. H.E. ×100.

Fig. 21. Early stage of intracerebral granuloma. Note the appearance of the characteristic large round cells at the subependymal zone. PID 16 from Group II. H.E. ×200.

Fig. 22. Early stage of intracerebral granuloma. Note the appearance of the large

306   K. JINNO

round cells, the beginning of inflammatory cell infiltration, and the small hemorrhagic focus around the ventricle (upper). PID 13 from Group I. H.E. ×200.

Fig. 23. Early stage of intracerebral granuloma. Note infiltration of inflammatory cells, mainly neutrophils, in the form of perivascular cuffings, associated with reactive gliosis in close contact with the ependymal cell layer (upper left). The proliferation of capillaries begins to occur. PID 14 from Group I. H.E. ×200.

Figs. 24-33. Electron microscopic findings of intracerebral granuloma.

Fig. 24. General view of the large round cells. Note abundant cytoplasm with large nucleus having prominent nucleolus. P, plasma cell. PID 27. ×5600.

Fig. 25. Large round cell. Fine fibrillar structures are well-developed in the cytoplasm of the large round cells. These fibrils about 70-90 Å in diameter are similar to gliofibrils and show parallel or intermingled arrangement. PID 17. (A) ×52600. (B) ×35000. (C) ×31900.

Fig. 26. Large round cell. Note abundant fibrils among increased numbers of intracytoplasmic organelles (Inset: ×39200). Irregularly indented nucleus, rough-surfaced endoplasmic reticulum and Golgi apparatus are also characteristic. Dense bodies (arrow) are occasionally seen. PID 17. ×21700.

Fig. 27. Many C-type virus particles are present in the intercellular space between the large round cells. PID 17. ×26200.

Fig. 28. C-type virus particles bud from the surface of the large round cells (arrows). PID 17. ×36700.

Fig. 29. Vascular wall. Many C-type virus particles are seen in the basal lamina and present also in the small vacuoles of the endothelium. PID 17. ×37600.

Fig. 30. Vascular wall. Virus particles are present in the basal lamina. PID 17. ×37600.

Fig. 31. Vascular channel in the virus-induced lesion. The virus particle is budding from the luminal cell membrane of the vascular endothelium. PID 17. ×75200.

Fig. 32. Large round cell. Virus particle is pinocytosed (viropexis) by the large round cell. PID 17. ×75200.

Fig. 33. Inflammatory cells. Note infiltration of three monocytes with numerous lysosomes and a neutrophil. PID 17. ×3750.

Fig. 34. Inflammatory cells. Note erythrophagia by a monocyte in the hemorrhagic area. PID 17. ×5000.

312   K. JINNO

314 K. Jinno

316   K. JINNO